Differentiating Cortical Areas Related to Pain Perception From Stimulus Identification: Temporal Analysis of fMRI Activity

A. VANIA APKARIAN,[1] ANEELA DARBAR,[1] BETH R. KRAUSS,[1] PATRICIA A. GELNAR,[1] AND NIKOLAUS M. SZEVERENYI[2]

Departments of [1]Neurosurgery and [2]Radiology, State University of New York Health Science Center, Syracuse, New York 13210

Apkarian, A. Vania, Aneela Darbar, Beth R. Krauss, Patricia A. Gelnar, and Nikolaus M. Szeverenyi. Differentiating cortical areas related to pain perception from stimulus identification: temporal analysis of fMRI activity. *J. Neurophysiol.* 81: 2956–2963, 1999. In a recent functional magnetic resonance imaging study (fMRI), we reported the cortical areas activated in a thermal painful task and compared the extent of overlap between this cortical network and those activated during a vibrotactile task and a motor task. In the present study we examine the temporal properties of the cortical activations for all three tasks and use linear systems identification techniques to functionally differentiate the cortical regions identified in the painful thermal task. Cortical activity was examined in the contralateral middle third of the brain of 10 right-handed subjects, using echo-planar imaging and a surface coil. In another eight subjects the temporal properties of the thermal task were examined psychophysically. The fMRI impulse response function was estimated from the cortical activations in the vibrotactile and motor tasks and shown to correspond to earlier reports. Given the fMRI impulse response function and the time courses for the thermal stimulus and the associated pain ratings, predictor functions were generated. The correlation between these predictor functions and cortical activations in the painful thermal task indicated a gradual transition of information processing anteroposteriorly in the parietal cortex. Within this region, activity in the anterior areas more closely reflected thermal stimulus parameters, whereas activity more posteriorly was better related to the temporal properties of pain perception. Insular cortex at the level of the anterior commissure was the region best related to the thermal stimulus, and Brodmann's area 5/7 was the region best related to the pain perception. The functional implications of these observations are discussed.

INTRODUCTION

Functional brain imaging studies show an extensive cortical network involved in human pain perception. The majority of these studies have been done with positron emission tomography (PET) using two-state subtraction techniques, i.e., subtracting brain images in a painful state from images collected in some control state (for example, see Casey et al. 1994; Jones et al. 1991; Talbot et al. 1991; for other references see review by Apkarian 1995). Recently we examined this network using functional magnetic resonance imaging (fMRI) and compared the spatial properties of the cortical responses in a thermal painful task to the responses to vibrotaction and motor performance (Gelnar et al. 1999). The study, in agreement with earlier studies, identified that a long list of cortical areas are involved in pain perception, either uniquely or partially overlapping with networks underlying vibrotaction and motor performance. Our assumption has been that these diverse cortical regions must be functionally specialized. Unlike PET, fMRI provides rich information regarding temporal fluctuations of the fMRI signal. Here we examine the temporal properties of the cortical fMRI responses in the thermal, vibrotactile, and motor tasks and use the temporal fluctuations of the cortical activity to functionally differentiate the cortical network underlying the responses to the thermal pain task.

Although there are multiple methods for acquiring functional brain activation information using magnetic resonance imaging (MRI), the blood oxygenation level–dependent contrast (BOLD-fMRI) remains the main tool for human brain mapping studies. The BOLD-fMRI signal detects decreases in local concentration of venous deoxyhemoglobin as an indirect measure of the local increase in neuronal or synaptic activity (Fox and Raichle 1986; Fox et al. 1988). BOLD-fMRI brain activation maps have been found to be consistent with cerebral blood flow based functional maps generated by PET (Clark et al. 1996; Ojemann et al. 1998) or by perfusion based MRI techniques (Kim 1995). A number of recent studies have shown that the BOLD-fMRI signal can be treated, within some limitations, as a linear time-invariant (LTI) system (Buckner et al. 1998; Cohen 1997; Friston et al. 1994; Rajapakse et al. 1998; Robson et al. 1998; Vazquez and Noll 1998). The main outcome of such a treatment of the BOLD-fMRI signal is the ability to characterize the hemodynamic impulse response function (IRF). This in turn can be convolved with an arbitrary input waveform to generate predictor functions with which the time courses of regional BOLD-fMRI signals can be differentiated (Cohen 1997). Another consequence of accepting that the BOLD-fMRI signal has LTI properties is the application of LTI systems identification techniques to fMRI data analyses.

In this study we use linear systems identification techniques to characterize the hemodynamic IRF in cortical fMRI responses to vibrotactile and motor tasks and show that these functions approximate those described by others. This step was necessary to justify the use of the canonical form as described by Cohen (1977) and to ensure that the hemodynamic response functions are not condition dependent. We also show, in a psychophysical experiment, that there is a prominent difference between the time course of the thermal stimulus and the associated pain perception. Once this dissociation is established, the brain activity is then probed with two predictor functions, one related to the stimulus and the second to the pain

The costs of publication of this article were defrayed in part by the payment of page charges. The article must therefore be hereby marked "*advertisement*" in accordance with 18 U.S.C. Section 1734 solely to indicate this fact.

perception. This approach tests the hypothesis that the regional cortical activities can be differentiated based on their correlations to the thermal stimulus or to the associated perception of the pain.

METHODS

Ten normal right-handed volunteers participated in the functional imaging study. Another eight right-handed subjects participated in the psychophysical study. The general purpose and the procedures were explained to the subjects. All subjects were at least 18 yr of age and gave written consent. The Institutional Review Board approved all procedures.

Functional imaging

Each individual underwent a single scanning session, which lasted ~1.5 h. It consisted of high-resolution anatomic scans in the sagittal and coronal planes, flow-weighted scans for identification of cortical vessels, and functional imaging series using echo-planar imaging (EPI) pulse sequences to quantify BOLD-based fMRI responses. Six subjects performed only the thermal painful task. In another four subjects, three separate functional series were done where the subjects performed either a motor, vibratory, or a thermal painful task. The spatial extent of the brain activations in these four subjects, combined with five other subjects, was described in our recent paper (Gelnar et al. 1999) (only subjects that underwent functional scans done with 1 NEX are included here, see below). Each control and stimulus state was 35 s in duration, and the subjects alternated between control and stimulus states for six control-stimulus cycles, for a total scan duration of 7 min. The stimulation methodology, scanning parameters, and data analysis approach are the same as those presented in detail in our recent papers (Gelnar et al. 1998, 1999). Briefly, the thermal painful stimulus consisted of alternately placing the right hand on either a surface heated to ~1°C above the subject's pain threshold or a warm surface (35°C). The vibrotactile stimulus was placing the right hand either on a surface vibrating at a dominant frequency of 50 Hz and maximum displacement of 2 mm or removing the hand from the vibrating surface. The motor task consisted of either sequential apposition of the first digit with the remaining digits of the right hand or rest. Switches between stimulus and control states were verbally cued.

The functional scans were performed on a 1.5-Tesla General Electric instrument equipped with echoplanar imaging capability. To improve signal-to-noise ratio, a single 5-in. circular surface coil was used, which was placed on the parietal cortex of the left brain. The subject's head was immobilized. Sagittal, high-resolution coronal and flow-weighted images were obtained with conventional pulse sequences. The functional images were obtained using the following echo planar pulse sequence: TR = 3,500 ms; TE = 60 ms; flip angle = 90°; NEX = 1 (number of averages per image); matrix = 256 × 128; FOV = 40 × 20 cm. This results in a voxel size of 1.56 × 1.56 × 6.00 mm. Ten images per slice location were collected during each control and stimulus state, acquiring 120 functional images in 6 cycles at 8 slice locations. Altogether this results in 960 functional images collected in each functional imaging series.

The primary cortical area of interest was the parietal cortex, so the middle third of the brain contralateral to the stimulation site was imaged, i.e., the posterior portion of the frontal cortex and most of the parietal cortex. Eight slice locations were selected for EPI functional scans (each 6.0 mm thick with a 0.5-mm gap between slices). In each study the first slice was located 6.0 mm posterior to the anterior commissure, and the last slice was 52.0 mm posterior to the anterior commissure.

Generating activation maps

The data analysis entailed the generation of activation maps in individual subjects. In-plane head movement was corrected by reregistering all images. An outlier detection routine was used to discard images with large deviations in mean count attributed to artifacts. Individual pixel unpaired *t*-test values were calculated for stimulus versus control conditions, using a cutoff criterion level of $P < 0.01$ for all tasks. A minimum cluster-size cutoff criterion of $P < 0.01$ was used to further limit significant activity. The latter defines the minimum number of contiguous pixels that pass the *t*-value cutoff. The overall false positive rate was calculated for these thresholds using the method of Xiong et al. (1995). The effective *P* value, which takes into account correction for multiple comparisons, was estimated to be between 0.02 and 0.0003. Pixels that survived both threshold criteria constituted the individual-subject activity map, i.e., clustered *t*-maps. These maps were superimposed on individual anatomic MR images and used to identify the locations of the activation clusters (significant regions of interest, ROIs). All significant ROIs, having at least eight contiguous pixels, located in the left frontal and parietal brain, were used in the time course analysis.

Activation time course analysis

The time course of the regional cortical activity was examined in the significant ROIs either by generating cycle-averaged responses (averaging the 6 serial control-stimulus cycles into a single cycle response) or by averaging all ROIs together. Assuming that these time curves are the output of an LTI system (Schwarz and Friedland 1965), we can calculate back the system's IRF, which defines the transfer function of cortical blood flow hemodynamics. Because the input (stimulus) can be approximated to a square waveform (35 s control and stimulus states), the output waveform (time course of each ROI) can be thought of as the step response function, i.e., the response to the convolution of the system's IRF when the input is a step function. According to LTI theory (Schwarz and Friedland 1965), the IRF is the time derivative of the step response function, which by definition is the output of the system when the input is a step function. This derivative can be approximated by calculating differences between consecutive time-step values of the step response. The resultant estimated IRFs were compared across tasks and to other studies.

Psychophysics of thermal pain perception

In the functional imaging study, only an overall single rating of the intensity of the pain was obtained at the end of the functional scan. Therefore the details of the time course of thermal pain perception were studied separately in a separate group of eight subjects. The same thermal stimulus used in the functional imaging studies was presented to the right hand. With the left hand the subjects continuously rated their pain perception, by manipulating a potentiometer. The potentiometer was connected to a chain of light-emitting diodes (LEDs) that had markings for different pain intensities. Five categories of pain intensities were designated. All LEDs being off was marked as no pain, three intermediate intensities, and all LEDs being on as maximum imaginable pain. This setup provides continuous visual feedback to the subject while rating perceived pain. The potentiometer output was digitized and fed to a personal computer for analysis. The group-averaged pain rating was generated representing the overall time course of pain perception for this thermal pain task in these subjects. This time curve was also assumed to delineate the mean pain perception for the subjects who performed the same task during functional scans.

Correlations with predictor functions

The average pain perception time curve was convolved with the cortical hemodynamic IRF, taken from Cohen (1997), to generate the predictor function for pain perception. Similarly, the stimulus time curve was convolved with the IRF to generate a predictor curve for the

stimulus. The correlation between significant ROIs in the thermal pain task and both predictor functions was evaluated: *CCs* and *CCp*, correlation coefficient for each ROI and stimulus and perception predictor curves, respectively. Also, the normalized relative distance, *d*, between the time curve of any ROI and the two predictor curves was evaluated, using

$$d = \frac{(CCs - CCp)}{(CCs + CCp)}$$

This quantity varies -1.0 and 1.0 since in all ROIs: $0 \leq CCs$ and $CCp \leq 1$. Negative values of this distance indicate that a given ROI is more closely related to the perception in comparison with the stimulus.

RESULTS

Hemodynamic impulse response function

The time course analysis was performed on all large, significant ROIs identified in the activation maps of the motor and vibrotactile tasks (4 subjects). Figure 1, *A–C*, illustrates activation time courses for the significant ROIs identified in the activation map of one subject performing the motor task. Each time curve is the six-cycle averaged activation of a distinct ROI. Time curves are shown for ROIs in the primary somatosensory (SI), secondary somatosensory (SII), cingulate, and insular cortices. The figure shows that the main difference between cortical areas is the magnitude of fMRI signal change with the time course remaining essentially invariant. Moreover, the rise and fall rates of the signal from the control-state to the stimulus-state and back are approximately the same. Similar symmetrical rise and fall rates were observed in the other subjects for the motor task and for the vibratory task.

Figure 1*D* shows the derivative of the six-cycle averaged activations for all ROIs in one subject performing the vibrotactile task. The derivatives are shown for each ROI as well as the average derivative. The rise and fall of this signal at the transitions from control state to the stimulus state and back approximate the time course of the IRF of blood hemodynamics in the cortex, and it is appropriately negative in the transition from the stimulus state to the control state.

The estimated hemodynamic IRF is shown in Fig. 2 for vibratory and motor tasks in three different subjects. The hemodynamic IRF for a visual task, from Cohen (1997), is also illustrated. A small number of data points characterize each estimated curve, which are limited by the sampling rate (TR = 3,500 ms determines the sampling rate). However, the estimated IRFs for the vibratory and motor tasks approximate the time course of the curve taken from Cohen (1997). From this correspondence we conclude that the hemodynamic IRF is not different among the three tasks and that we can use the IRF from the visual task to generate various predictor functions.

Time course of thermal pain perception

The details of the pain perception associated with the thermal painful task were examined psychophysically in eight subjects. Individual-subject pain perception ratings are presented for all eight subjects in Fig. 3*A*. The group-mean perception of the thermal pain is also shown in Fig. 3*B*. The figure illustrates that, in every stimulus cycle, pain perception con-

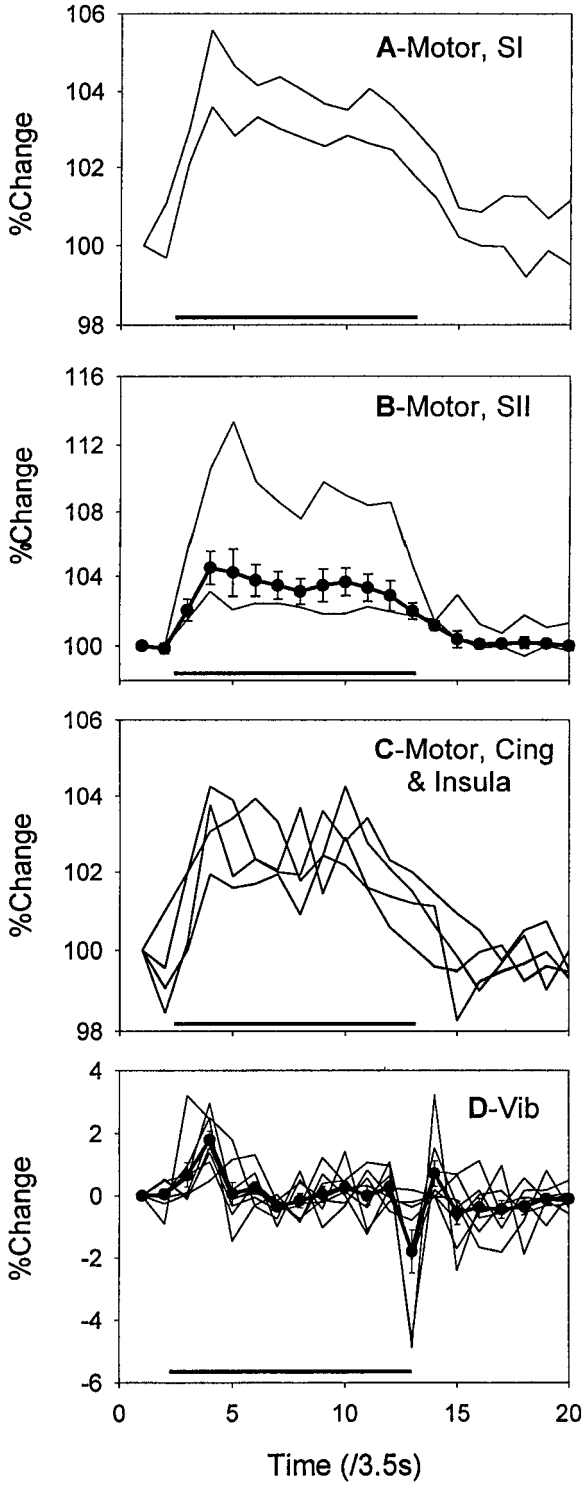

FIG. 1. Time course of activations and their time derivatives. *A–C*: activations for all regions of interest (ROIs) examined in the middle third of the contralateral brain in a subject performing right hand finger apposition task. *D*: time derivative of cortical activations in another subject performing a vibrotactile task. In *A–C* each curve is the time course of a single ROI. Two ROIs were located in primary somatosensory cortex (SI; *A*), 2 in secondary somatosensory cortex (SII; *B*), and 4 in cingulate and insular regions (*C*). The mean ± SD of these 8 ROIs is shown in *B* (large filled dots with error bars). The percentage change activations are the mean changes when all 6 control and stimulus cycles are averaged, and the MR signal in the 9th control image is set to 100%. *D*: time derivatives of the 6-cycle averaged activations are shown for all ROIs. Large filled circles with error bars are the average of all the derivatives. Thick lines on the *x*-axes indicate stimulus periods.

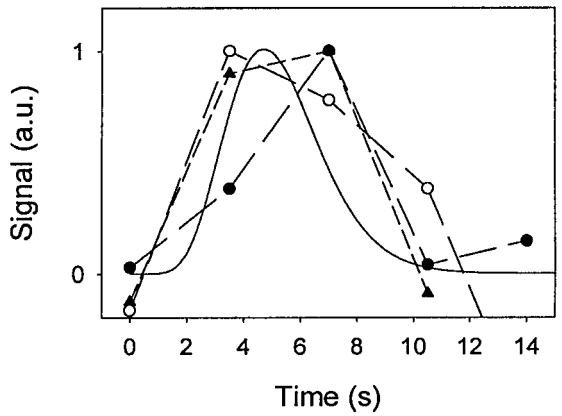

FIG. 2. Estimated impulse response function for the brain functional magnetic resonance imaging (fMRI) signal measured for 3 different tasks. The 3 curves connecting different symbols were generated from the time derivatives of the control-stimulus transitions of 6-cycle averaged cortical activations for all ROIs examined in 3 subjects. Filled and unfilled circles are from 2 subjects performing the vibrotactile task. Filled triangles are from another subject performing the motor task. The continuous curve is the impulse response function taken from Cohen (1997), which is a gamma function $\mathrm{IRF}(t) = 0.452 * t^{8.6} * \exp(-t/0.547)$, where t is time in seconds, fitted to the fMRI response to 10 repetitions of a 1-s light flash stimulus measured in the visual cortex.

tinuously increases for the duration of the application of the thermal stimulus, resulting in a large difference between the rise rates and fall rates of perception. Moreover, the peak pain ratings show an initial habituation (between 1st and 2nd cycles), followed by sensitization. It should be emphasized that the stimulus temperature (measured on the skin) stabilizes within 5 s after placing the hand on the painful surface. Therefore there is a large dissociation between the time characteristics of the thermal stimulus and the perceived pain.

Average cortical activity in the thermal pain task and predictor functions

In the thermal painful task, the time course of different ROIs was more variable in comparison with the time courses for ROIs observed in the vibrotactile and motor tasks. This observation, in fact, was the initial impetus for undertaking the current study. To characterize the overall time course of the cortical activation in the thermal pain task, the cortical activations in all ROIs, 45 ROIs in 10 subjects, were normalized and averaged. This across regions and subjects averaged time course of cortical activation is shown in Fig. 4. Figure 4 also shows the time course of the thermal stimulus convolved with the hemodynamic IRF (stimulus predictor function) and the average pain perception convolved with the hemodynamic IRF (perception predictor function). Clearly all three curves are highly interrelated. The correlation coefficients among the three curves were 0.82 ($P < 10^{-29}$) between the overall cortical activity and stimulus predictor curve, 0.75 ($P < 10^{-21}$) between the stimulus and perception predictor curves, and 0.62 ($P < 10^{-14}$) between overall cortical activity and perception predictor curve. Thus the average time course of the cortical activation in the thermal pain task is more closely correlated to the stimulus than to the perception predictor curve.

The average cortical activation curve leads the other two curves at the beginning of each stimulus cycle. Moreover, in most cycles it peaks just before the stimulus predictor curve reaches its maximum. It is interpreted that this early component of the activation curve is due to the motor task necessary in the initiation of the stimulus cycle: moving the hand from the warm surface to the hot surface. On the other hand, in the later phase of each stimulus cycle, the average activation curve shows a good correspondence with the peak of the perception predictor curve. There is also a baseline shift in the cortical activation curve that remains unexplained.

Regional differences in correlations with predictor functions

Correlation coefficients were calculated between the time curve of each ROI in the thermal task and the stimulus and perception predictor curves, CCs and CCp, respectively. Across all ROIs, CCs was larger than CCp (paired t-test, $t = 8.83$, $P < 0.001$). Figure 5*A* shows the distribution of CCp as a function of brain slice locations where the respective ROIs were found. The magnitude of CCp increases with slice location number, i.e., more posteriorly within the middle third of the brain. Linear regression analysis results in statistically significant dependence of CCp on slice location ($R = 0.49$, $F = 13.7$, $P < 0.001$). A similar pattern was seen for CCs (not shown) with statistically significant dependence on slice location (linear regression analysis, $R = 0.4$, $F = 8.5$, $P < 0.01$).

The distance, d, that characterizes the relative distance of the

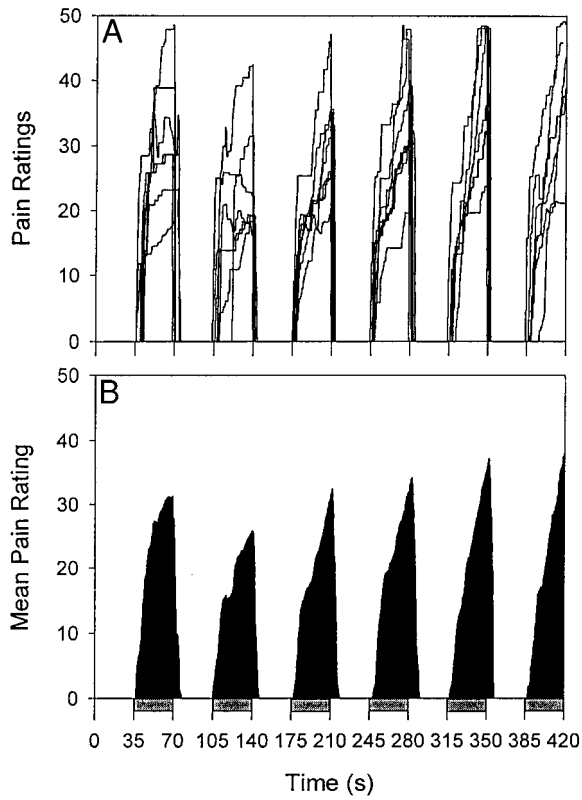

FIG. 3. Pain perception ratings for the thermal task in 8 subjects. *A*: individual subject ratings. *B*: group-averaged pain ratings. Gray bars indicate the cycles where the hand was placed on the painfully hot surface (stimulus). The pain rating scale included 5 categories 0 was designated as no pain, 12 as mild pain, 25 as moderate pain, 37 as severe pain, and 50 as maximum imaginable pain.

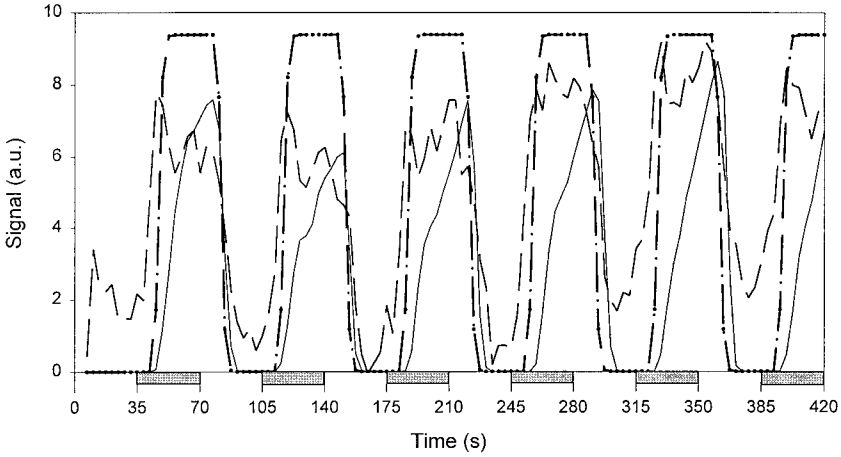

FIG. 4. Relationship between the average fMRI activation in the thermal pain task with the stimulus predictor and perception predictor curves. The solid line is the predictor function for pain perception generated by convolving the group averaged pain rating (Fig. 3*B*) with the fMRI impulse response function (IRF; solid line in Fig. 2). Dash-dotted thick line is the predictor function for the thermal stimulus generated by convolving the stimulus (shown with gray bars on the *x*-axis) with the fMRI IRF. Dashed line is the normalized average cortical activation for the thermal pain task across 45 ROIs in 10 subjects. The *y*-axis is in arbitrary units (a.u.).

time curve of a given ROI from the stimulus and perception predictor curves was analyzed as a function of slice location of each ROI (Fig. 5*B*). Only 3 of 45 ROIs had negative *d* values, implying that the time course of these ROIs was more similar to the perception rather than to the stimulus predictor curve. More importantly, the magnitude of *d* decreased with slice location number (linear regression analysis, $R = 0.57$, $F = 20.2$, $P < 0.001$), implying that the regional cortical activations were relatively better related to the perception predictor curve more posteriorly than anteriorly, within the brain region studied.

The three largest values of *d*, found in slice 0, were all located in the insular cortex (Fig. 5*B*). On the other hand the *d* values calculated for the ROIs found in slice 6 were all located in Brodmann's area 5/7. Values of *d* intermediate to these extremes were localized to the motor and somatosensory cortical regions spanning the parietal cortex, namely, premotor cortex, cingulate and supplementary motor cortex, primary motor cortex, primary and secondary somatosensory cortex, and Brodmann's area 40.

DISCUSSION

The main result of this study is the demonstration that the time course of the fMRI-BOLD signal can be used to functionally parcel brain regions by testing the extent to which different cortical activations correspond to one shape of time course versus another, i.e., by the use of predictor functions. The two functions were generated from the thermal stimulus properties and the group-averaged ratings of the consciously perceived pain. The underlying assumption is the presence of various information-processing stages in the cortex where stimulus properties are transformed into conscious perception properties. The current analysis confirms this principle because it shows a highly statistically significant dependence of the location of a given cortical activation with the relative correlation with the perception and stimulus predictor functions. Moreover, the results show that the more posterior regions of the parietal cortex better reflect the time properties of pain perception. This observation in general is consistent with the cortical hierarchy of somatosensory representation. Anatomic and physiological studies indicate that the primary somatosensory cortical neuron properties correspond more closely to stimulus properties than higher somatosensory cortical areas, which are found in more posterior parietal regions of the cortex (Kaas 1993).

The observation that the insular cortical activity best reflects the stimulus parameters implies that this region most likely is involved in the preferential coding of the temperature characteristics of the stimulus. This result is consistent with recent observations by Craig et al. (1996), where the cortical activation sites for a thermal illusion of pain was studied. A major result of that study was the illustration that part of the insula, anteroposteriorly located at the anterior commissure, was the only cortical region activated by all noxious and innocuous thermal stimuli (5°C, 20°C, grill, 40°C, and 47°C were tested). The cortical activities exhibiting the highest *d* values in our study are located in this same part of the insula. Thus our results agree with Craig et al.'s assessment that this region is involved in monitoring the thermal status of the body. This conclusion is also consistent with our earlier spatial analysis of the cortical activations (Gelnar et al. 1999), where we showed that this part of the insula was activated only during the thermal painful task, and it was not activated during vibrotactile or motor tasks.

In contrast to the insula, the more posterior regions of the parietal cortex and specifically area 5/7 seems more related to the perceived pain. This observation is consistent with both human cortical lesion data and monkey electrophysiological results. Studies of nociceptive neurons in area 7b in the awake monkey indicate that these cells have highly complex response properties attributed to spatial multimodal and multisensory convergence (Dong et al. 1989, 1994). The latter is consistent with our earlier results (Gelnar et al. 1999), showing that this region is activated during multiple sensory and motor tasks (thermal pain, vibrotaction, and motor performance). In contrast to nociceptive cells in the primary somatosensory cortex, those in area 7b do not encode stimulus location and intensity with high fidelity. Moreover, the stimulus-response properties of some of these nociceptive cells closely approximate the stimulus intensity–escape frequency function (Dong et al. 1994). Thus these nociceptive neurons seem to be the only ones found in the cortex that have response characteristics that in the human would be described as related to the perception of pain. Cortical lesions in and around the region, especially in the white matter underlying the posterior parietal cortex can give

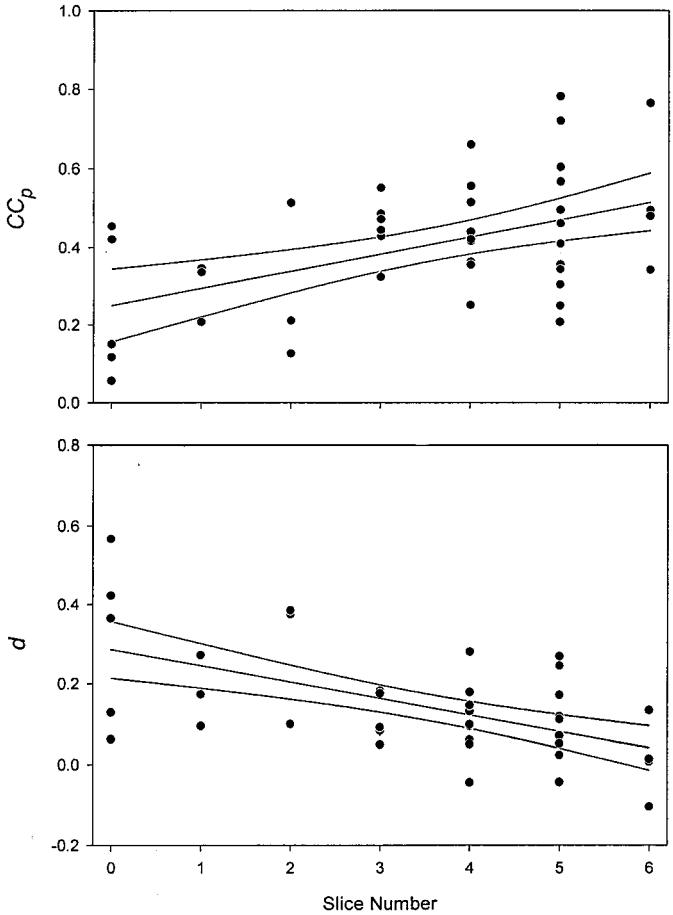

FIG. 5. Relationship between perception and stimulus predictor functions and the anteroposterior location of cortical activation ROIs in the thermal pain task. *A*: magnitude of the correlation coefficient between the perception predictor curve and each cortical activation in the thermal pain task (CCp) as a function of the slice location where the cortical activation ROIs were located. *B*: relative distance (*d*) for each cortical activation in the thermal pain task from the stimulus predictor and perception predictor curves as a function of the slice location where the cortical activation ROI was located. The linear regression lines and the corresponding 95% confidence intervals are shown for both graphs. In all 10 subjects, 8 contiguous coronal slices were scanned such that slice 0 was centered 6 mm posterior to the anterior commissure, and subsequent slices were separated from each other by 6.5 mm.

rise to pain perception abnormalities in monkeys (Dong et al. 1996) and in humans (Berthier et al. 1988; Greenspan and Winfield 1992; Salanova et al. 1995; Schmahmann and Liefer 1992). The studies in one monkey (Dong et al. 1996) and in one human (Greenspan and Winfield 1992) have indicated that, although trauma to the posterior parietal cortex increases thermal pain tolerance, thermosensitivity may remain intact. The latter again reinforces our functional parcellation of the parietal cortex into a temperature monitoring region and a pain perception region. The clinical studies indicate that lesions in the posterior parietal cortex can give rise to pain asymbolia (neglect), hypoalgesia, analgesia, and spontaneous pain. Therefore our results taken together with the clinical lesion observations and the response properties of cells in the posterior parietal cortex imply that the region may be uniquely involved in the conscious subjective experience of pain.

It should be mentioned that the causal relationship between the stimulus predictor function and the cortical activity is less clear for the areas with *d* values intermediate to those observed for the insula and area 5/7. This is primarily due to a motor confounder because the subjects had to move the hand to receive the thermal stimulus. As a result, the average cortical response to the thermal stimulus contained an initial response leading the stimulus predictor function. Thus the stimulus predictor function is also partially a predictor for the hand movement. Because the more intermediate portion of the brain region studied encompasses primary, pre-, and supplementary motor, as well as primary somatosensory and other cortical regions, the distinction between stimulus identification and hand movement remains unresolved for these regions. Moreover, we expect that the differentiation along the stimulus-perception dimension for pain may become more pronounced in these regions when the motor confounder is eliminated.

The approach used here is, in some ways, similar to a recent fMRI study that examined the cortical network underlying working memory (Courtney et al. 1998). By using different time course patterns of the fMRI signal as regressors, the authors functionally subdivide the cortical activity into regions involved in responding to nonselective visual stimuli, face selective responses, and working memory responses. Moreover, they show that the extent of involvement changes continuously across six regions of the cortex, similar to the continuum we show for the involvement of the parietal cortical activity in the perception of pain.

The other major conclusion of the study is the demonstration that the time scale of pain perception variation (seconds to minutes) matches the scale of the cortical IRF. Thus, although BOLD-fMRI time course is very slow relative to neuronal activity (milliseconds), the temporal component of BOLD-fMRI seems to be an ideal tool with which brain regions can be differentiated relative to a stimulus and its painful perception dimensions. The slow changes in conscious pain perception are due to peripheral mechanisms, like slow transmission through unmyelinated fibers or thinly myelinated fibers, and central mechanisms, such as long afterdischarges in central nociceptive cells (Willis 1985). These slow changes, where the pain intensity seems to continuously increase in time even though the temperature on the skin is constant, are unique to the pain sensory system. In contrast, the touch sense shows a dramatic adaptation to a constant stimulus (e.g., one's perception of the clothes they are wearing), whereas in vision there is a constancy of perception (images do not fade when one fixates on them).

The nociceptive input to the cortex arrives relatively quickly. Laser heat stimulation evoked potential studies show a cortical event around 170 ms after the stimulus (Treede et al. 1995). In comparison, electrical median nerve stimulation evoked potentials (mediated through large fibers signaling innocuous cutaneous information) reach the cortex in 20 ms. Although the thermal evoked potentials are delayed by 150 ms from the innocuous potentials, this delay is not significant relative to the cortical IRF, which peaks at 5 s. There is an even later potential, called ultra-late laser evoked potential (Treede et al. 1995). Its latency is 1,500 ms, which seems to be due to the activation of unmyelinated nociceptive fibers. However, this ultra-late potential is also too short relative to the cortical IRF. The evoked potentials measure the time for the initial arrival of neuronal volley to the cortex. Its time course is very different from the conscious pain perception, which continuously changes over 35 s in our task. The large temporal

difference between detecting the first cortical activity and the conscious perception of pain further reinforces the notion that the early cortical activity is more related to the stimulus dimensions. Moreover, this large difference in the arrival of nociceptive inputs and pain perception strongly implies that the changes in perception are primarily based on central properties.

The results of the present study show that the BOLD-fMRI signal has a characteristic hemodynamic IRF that is similar among different tasks: vision, vibrotaction, and motor performance, and across subjects. By using this IRF function to examine the time course of cortical activity in the thermal stimulus and its perception, we indirectly also show that this IRF is applicable to pain-inducing tasks. Further, the successful use of linear systems identification techniques reinforces the assumption that BOLD-fMRI signal follows LTI properties as long as the stimulus properties are limited to the linear range of fMRI responses (Robson et al. 1998; Vazquez and Noll 1998).

Conclusions

By examining the time course of pain perception in a stereotyped thermal pain task, it was shown that the stimulus and perception significantly differ from each other. We take advantage of this time course difference and, by using linear systems identification techniques, demonstrate that the more posterior regions of the middle third of the brain seem to be relatively better correlated with the perceived pain as compared with the applied thermal stimulus. It should be noted that all earlier brain imaging studies of pain have implicitly assumed that the stimulus properties are sufficient to define pain perception and to identify brain areas involved in pain perception. Given the limitations of the experimental design of the current study, we restricted the cortical spatial analysis of the differentiation between stimulus and perception to the anteroposterior dimension. The more detailed anatomic differentiation of the cortical network underlying pain in relation to stimulus properties versus pain perception are postponed to future studies, where painful stimuli are applied without moving the hand, the time variations of each subject's pain perception is used to generate individual predictor curves (rather than the group averaged perception), and more areas of the brain are included in the functional scans. Our recent studies are designed to accomplish these improvements.

The authors thank A. Armstrong for contributions in the psychophysical studies. We also thank S. Huckins and G. Tillapaugh-Fay for assistance with functional MR data collection, and M. Fonte for functional MRI data analysis software development.

This study was funded by National Institute of Neurological Disorders and Stroke Grant NS-35115 and by the Department of Neurosurgery at State University of New York Health Science Center.

Address for reprint requests: A. V. Apkarian, Neurosurgery Research Labs, SUNY Health Science Center, 766 Irving Ave., Syracuse, NY 13210.

Received 24 December 1998; accepted in final form 2 February 1999.

REFERENCES

APKARIAN, A. V. Functional imaging of pain: new insights regarding the role of the cerebral cortex in human pain perception. *Semin. Neurosci.* 7: 279–293, 1995.

BERTHIER, M., STARKSTEIN, S., AND LEIGURDA, R. Asymbolia for pain: a sensory-limbic disconnection syndrome. *Ann. Neurol.* 24: 49, 1988.

BUCKNER, R. L., KOUTSTAAL, W., SCHACTER, D. L., DALE, A. M., AND ROTTE, M. Functional-anatomic study of episodic retrieval. II. Selective averaging of event-related fMRI trials to test the retrieval success hypothesis. *Neuroimage* 7: 163–175, 1998.

CASEY, K. L., MINOSHIMA, S., BERGER, K. L., KOEPPE, R. A., MORROW, T. J., AND FREY, K. A. Positron emission tomographic analysis of cerebral structures activated specifically by repetitive noxious heat stimuli. *J. Neurophysiol.* 71: 802–807, 1994.

CLARK, V. P., KEIL, K., MAISONG, J., COURTNEY, S., UNGERLEIDER, L. G., AND HAXBY, J. V. Functional magnetic resonance imaging of human visual cortex druing face matching: a comparison with positron emissions tomography. *Neuroimage* 4: 1–15, 1996.

COHEN, M. S. Parametric analysis of fMRI data using linear systems methods. *Neuroimage* 6: 93–103, 1997.

COURTNEY, S. M., UNGERLEIDER, L. G., KEIL, K., AND HAXBY, J. V. Transient and sustained activity in a distributed neural system for human working memory. *Nature* 386: 608–611, 1998.

CRAIG, A. D., REIMAN, E. M., EVANS, A., AND BUSHNELL, M. C. Functional imaging of an illusion of pain. *Nature* 384: 258–260, 1996.

DONG, W. K., CHUDLER, E. H., SUGIYAMA, K., ROBERTS, V. J., AND HAYASHI, T. Somatosensory, multisensory, and task-related neurons in cortical area 7b (PF) of unanesthetized monkeys. *J. Neurophysiol.* 72: 542–564, 1994.

DONG, W. K., HAYASHI, T., ROBERTS, V. J., FUSCO, B. M., AND CHUDLER, E. H. Behavioral outcome of posterior parietal cortex injury in the monkey. *Pain* 64: 579–587, 1996.

DONG, W. K., SALONEN, L. D., KAWAKAMI, Y., SHIWAKU, T., KAUKORANTA, E. M., AND MARTIN, R. F. Nociceptive responses of trigeminal neurons in SII-7b cortex of awake monkeys. *Brain Res.* 484: 314–324, 1989.

FOX, P. T. AND RAICHLE, M. E. Focal physiological uncoupling of cerebral blood flow and oxidative metabolism during somatosensory stimulation in human subjects. *Proc. Natl. Acad. Sci. USA* 83: 1140–1144, 1986.

FOX, P. T., RAICHLE, M. E., MINTUN, M. A., AND DENCE, C. Nonoxidative glucose consumption during focal physiologic neural activity. *Science* 241: 462–464, 1988.

FRISTON, K. J., JEZZARD, P., AND TURNER, R. Analysis of functional MRI time-series. *Hum. Brain Mapping* 1: 153–171, 1994.

GELNAR, P. A., KRAUSS, B. R., SHEEHE, P. R., SZEVERENYI, N. M., AND APKARIAN, A. V. A comparative fMRI study of cortical representations for thermal painful, vibrotactile, and motor performance tasks. *Neuroimage.* In press.

GELNAR, P. A., KRAUSS, B. R., SZEVERENYI, N. M., AND APKARIAN, A. V. Fingertip representation in the human somatosensory cortex: an fMRI study. *Neuroimage* 7: 261–283, 1998.

GREENSPAN, J. D. AND WINFIELD, J. A. Reversible pain and tactile deficits associated with a cerebral tumor compressing the posterior insula and parietal operculum. *Pain* 50: 29–39, 1992.

JONES, A.K.P., BROWN, W. D., FRISTON, K. J., QI, L. Y., AND FRACKOWIAK, R.S.J. Cortical and subcortical localization of response to pain in man using positron emission tomography. *Proc. R. Soc. Lond. B Biol. Sci.* 244: 39–44, 1991.

KAAS, J. H. The functional organization of somatosensory cortex in primates. *Anatomischer Anzeiger.* 175: 509–518, 1993.

KIM, S.-G. Quantification of relative cereral blood flow change by flow-sensitive alternating inversion recovery (FAIR) technique: application to functional mapping. *Magn. Reson. Med.* 34: 293–301, 1995.

OJEMANN, J. G., BUCKNER, R. L., AKBUDAK, E., SNYDER, A. Z., OLLINGER, J. M., MCKINSTRY, R. C., ROSEN, B. R., PETERSEN, S. E., RAICHLE, M. E., AND CONTURO, T. E. Functional MRI studies of word-stem completion: reliability across laboratories and comparison to blood flow imaging with PET. *Hum. Brain Mapping* 6: 203–215, 1998.

RAJAPAKSE, J. C., KRUGGEL, F., MAISOG, J. M., AND VON CRAMON, D. Y. Modeling hemodynamic response for analysis of functional MRI time-series. *Hum. Brain Mapping* 6: 283–300, 1998.

ROBSON, M. D., DOROSZ, J. L., AND GORE, J. C. Measurements of the temporal fMRI response of the human auditory cortex to trains of tones. *Neuroimage* 7: 185–198, 1998.

SALANOVA, V., ANDERMANN, F., RASMUSSEN, T., OLIVER, A., AND QUESNEY, L. F. Parietal lobe epilepsy. Clinical manifestations and outcome in 82 patients treated surgically between 1929 and 1088. *Brain* 118: 607–627, 1995.

SCHMAHMANN, J. D. AND LEIFER, D. Parietal pseudothalamic pain syndrome, clinical features and anatomic correlates. *Arch. Neurol.* 49: 1032–1037, 1992.

SCHWARZ, R. J. AND FRIEDLAND, B. *Linear Systems.* New York: McGraw-Hill, 1965.

TALBOT, J. D., MARRETT, S., EVANS, A. C., MEYER, E., BUSHNELL, M. C., AND DUNCAN, G. H. Multiple representation of pain in human cerebral cortex. *Science* 251: 1355–1358, 1991.

TREEDE, R.-D., LORENZ, J., KUNZE, K., AND BROMM, B. Assessment of nociceptive pathways with laser-evoked potentials in normal subjects and patients. In: *Advances in Pain Research and Therapy*, edited by B. Bromm and J. E. Desmedt. New York: Raven, 1995, p. 377–392.

VAZQUEZ, A. L. AND NOLL, D. C. Nonlinear aspects of the BOLD response in functional MRI. *Neuroimage* 7: 108–118, 1998.

WILLIS, W. D. *The Pain System. The Neural Basis of Nociceptive Transmission in the Mammalian Nervous System.* Basel: Karger, 1985.

XIONG, J., GAO, J. H., LANCASTER, J. L., AND FOX, P. T. Clustered pixels analysis for functional MRI activation studies of the human brain. *Hum. Brain Mapping* 3: 287–301, 1995.